A Novel Composite Nano-scaffold with Potential Usage as Skin Dermo-epidermal Grafts for Chronic Wound Treatment

Sohrab Moradi[1], Mohammad Ali Nilforoushzadeh[2], Jamil Zargan[1], Shahram Nazarian[1, *] and Peiman Brouki Milan[3, **]

[1]Department of Biology, Faculty of Basic Science, Imam Hossein University, Tehran, Iran
[2]Skin and Stem cell Research Center (SSRC), Tehran University of Medical Sciences, Tehran, Iran
[3]Department of Tissue Engineering & Regenerative Medicine, Faculty of Advanced Technologies in Medicine, Iran University of Medical Sciences, Tehran, Iran

[*]*Corresponding author*: Department of Biology, Faculty of Basic Science, Imam Hossein University, Tehran, Iran. Email: kpnazari@ihu.ac.ir
[**]*Corresponding author*: Department of Tissue Engineering & Regenerative Medicine, Faculty of Advanced Technologies in Medicine, Iran University of Medical Sciences, Tehran, Iran. Email: brouki.p@iums.ac.ir

Abstract

Background: Nano-scaffolds loaded with bioactive compounds such as ZnO nanoparticles (ZnO-NPs), as tissue-engineered artificial skin grafts, can be a suitable substitute for extracellular matrix and greatly contribute to accelerating chronic wound treatment by decreasing the chance of bacterial infection.

Methods: Silk fibroin nanofiber was fabricated by using electrospinning and three-dimensional porous hybrids (3DPH) nano-scaffold with composite of sodium alginate/ZnO-NPs solution and silk fibroin electrospun nanofibers by adopting freeze-drying method. Successful configuration of nanofibers and porous nano-scaffolds were confirmed using field emission scanning electron microscopy (FE-SEM). Antimicrobial activity, cell attachment, and cytotoxicity evaluation of scaffolds were performed by employing disk diffusion method, L929 cell culture, and MTT assay, respectively.

Results: Antibacterial analysis of 3DPH nano-scaffolds revealed their appropriate antibacterial activity against the *Staphylococcus aureus* and the *Escherichia coli* bacteria. Furthermore, the results from cytotoxicity and cell adhesion analyses indicated the appropriate cell attachment, viability, and proliferation on the silk fibroin nanofibers and 3DPH nano-scaffold, which are fundamental for wound healing and skin dermo-epidermal grafts.

Conclusions: In sum, silk fibroin nanofiber as an epidermal graft and 3DPH nano-scaffold loaded with ZnO-NPs as a dermal graft were fabricated. Moreover, 1.5% (w/v) concentrations of ZnO-NPs were selected and incorporated into the 3DPH nano-scaffold. Considering the promising results of biological analyses, the nanofibrous and 3DPH nano-scaffolds composite may have been suitable for skin dermo-epidermal grafts and skin regeneration.

Keywords: Silk Fibroin Nanofiber, Electrospinning, 3DPH Nano-scaffold, Dermo-epidermal Grafts

1. Background

As the largest organ system in the body, the skin plays a crucial role in multiple important physiological functions. Compromising the skin's integrity by injury or illness can lead to physiologic imbalances, chronic wounds, and, occasionally, even death (1). Depending on the healing duration, the wound may be classified as acute or chronic. Chronic wounds, unlike acute wounds, cannot heal at an expected timeframe because they do not progress beyond the inflammatory phase, preventing the proliferation of vascular endothelial cells and fibroblasts as well as the deposition of collagen matrix (2). Chronic wounds are usually treated with autografts, allografts, xenografts, and topical antibacterial and anti-inflammatory agents. Neverthe-

less, the above therapies are not sufficient for extensive or deep wounds (3). Autografts are most advantageous because they do not exhibit immune responses, but they cannot cover the entire wounded site when it exceeds 60% of the patient's total body area. Additionally, the application of allogeneic skin grafts carries a high risk of rejection and treatment failure (3, 4). Modern treatments include skin tissue engineering, which produces bioengineered biomaterial-based artificial skin grafts aimed at overcoming the shortage of donor skin graft supplies as well as the rejection of skin allografts and xenografts (5). Moreover, bioengineered artificial skin substitutes are becoming more popular for treating chronic wounds and for topical delivery of mesenchymal stem cells to reduce in-

flammation and speed healing (5, 6). Artificial skin grafts with pre-seeded cells or cells incorporated within the matrix are known as cellular artificial skin grafts, while those with or without cells are known as acellular artificial skin grafts (6). The main roles of bioengineered skin grafts are to prevent infections, keep the wound from dehydration, supply oxygen, and promote healing (6, 7). Depending on their anatomical structure, similar to autologous skin transplants, artificial skin substitutes may be categorized as epidermal, dermal, or dermo-epidermal (8, 9). A scaffold is an essential component of skin tissue engineering and artificial skin grafts since it has a pivotal role in mechanical support, delivery of nutrients and oxygen, as well as the release of growth factors and drugs. It can also modulate cell behaviors such as attachment, motility, proliferation, and differentiation. Therefore, scaffolds could mimic the biological, chemical, and mechanical properties of the extracellular matrix (ECM) of the target tissue. Several types of scaffolds can be utilized for artificial skin grafts, including fibrous, porous, and hydrogel scaffolds (10, 11).

2. Objectives

The current study aimed to design two nano-scaffolds, fibrous and porous, as skin dermo-epidermal grafts with silk fibroin (SF), sodium alginate (SA), and ZnO nanoparticles (ZnO-NPs) (Figure 1). Silk fibroin nanofiber is fabricated by electrospinning as an epidermal graft and three-dimensional porous hybrids (3DPH) nano-scaffold loaded with ZnO-NPs by adopting the freeze-drying method as a dermal graft.

3. Methods

3.1. Materials

Silkworm (*Bombyx mori*) cocoons (i.e., a generous gift from Iran Silkworm Research Center, Guilan, Iran), sodium alginate ($C_6H_9NaO_7$, High MW, Merck, Germany), ZnO-NPs (Nanozino company, Iran), Dulbecco's modified Eagle's medium (DMEM), fetal bovine serum (FBS), phosphate buffered saline (PBS), penicillin-streptomycin (P/S) (Bio-Idea, Iran), lithium bromide (LiBr, VWR Prolab, Belgium), polyethylene oxide (PEO) (Merck, Germany), sodium carbonate (Na_2CO_3, Merck, Germany), 98% formic acid (HCOOH, Merck, Germany), and calcium chloride ($CaCl_2$, Merck, Germany) were used in this study.

3.2. ZnO Nanoparticles

In this study, oval and quasi-spherical shaped nanoparticles with an average diameter of 35 ± 10 nm were used irregularly. In addition, the crystalline structure of ZnO-NPs

was hexagonal and high purity without any other phase impurities. The zeta potential of ZnO-NPs in DDW was equal to -16.8 mV, implying a stable colloidal solution.

3.3. Silk Fibroin Extraction

Silk fibroin solution was prepared with a concentration of 8 - 10% (w/v) according to the protocol of Vepari and Kaplan (12). The 3 - 4 *B. mori* cocoons were boiled in 1 liter of 0.02 M aqueous sodium carbonate (Na_2Co_3) solution for 45 minutes and rinsed with water in order to remove sericin. The degummed silk was dried overnight and dissolved in 9.3 M LiBr solution (in a ratio of 8 - 10% silk weight) for four hours on a heater stirrer at 55°C. After filtration of SF solution, it was dialyzed against distilled water for 48 h. Finally, the extracted silk fibroin was lyophilized by electrospinning using the freeze-drying method.

3.4. Fabrication of Nanofibers by Electrospinning

Silk fibroin fibrous scaffolds were fabricated adopting electrospinning. To fabricate the SF nanofibers, 8% (w/v) SF solution was dissolved in formic acid (98%). To complete the electrospinning process, the voltage electric field, flow rate, and collector distance were applied at 18 kV, 1 ml/h, and 13 cm, respectively.

3.5. Fabrication of Three-dimensional Porous Hybrid Nanoscaffolds

The main solution, SA/ZnO-NPs suspension, was prepared using 0.5% (w/v) of SA and different concentrations of ZnO-NPs (0.5, 1, 1.5, and 2% (w/v)) in deionized water. The suspension was homogenized by stirrer vigorously for 15 min and ultrasonic vibration for 15 min. Then, 1 mg/mL solution of cut about 3 - 4 mm² electrospun SF nanofibers was prepared in deionized water, performing vortex for 15 min and ultrasonic vibration for 15 min. The final solution was prepared using blend of main and SF nanofibers solutions with 1: 3 ratio and mixing them by thoroughly stirring for 1 hour to obtain a homogenous mixture. The 3DPH nanoscaffolds were fabricated by implementing freeze-drying (EYELA, FD1) under -40°C temperature of condenser and applying 8.5 - 9 Pa pressure for 24h. The porous film was immersed in 1% (w/v) $CaCl_2$ for 2 h in order to induce crosslink.

3.6. Electron Microscopic Analysis

The surface morphology of nano-scaffolds was examined using field emission scanning electron microscopy (FE-SEM; TESCAN-MIRA3, Czech Republic) with voltage and amperage of 15 - 50 kV and 2 - 10 μA, respectively.
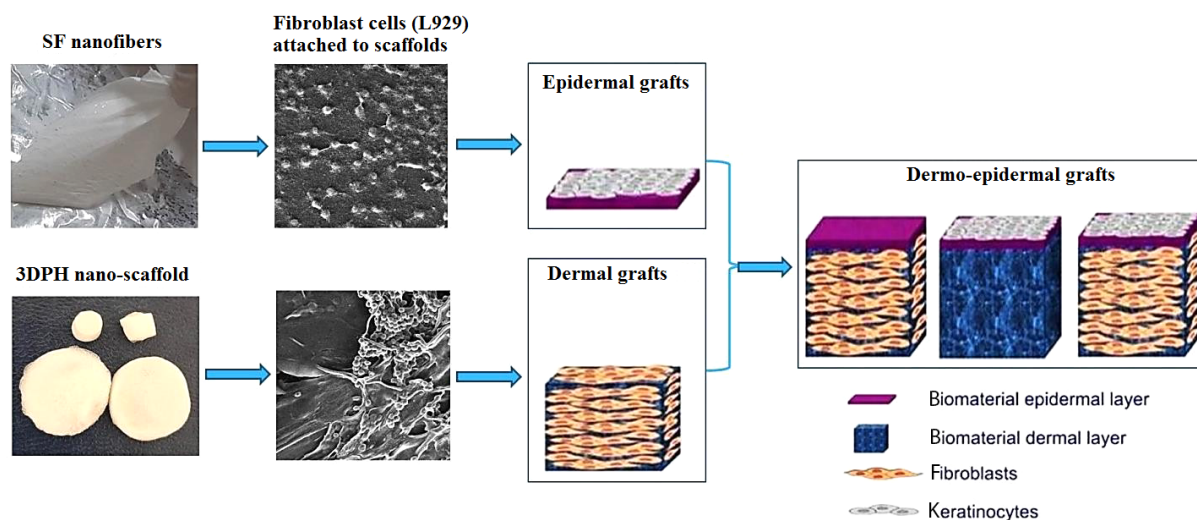
Figure 1. The graphical abstract and overview of objectives

3.7. Biological Activity Assessment of Nano-scaffolds

The antibacterial activity of 3DPH nano-scaffolds loaded with 0.5, 1, 1.5, and 2% (w/v) ZnO-NPs was evaluated against the *Staphylococcus aureus* and *Escherichia coli* bacteria by disk diffusion assay according to the European Committee on Antimicrobial Susceptibility Testing (EUCAST) guidelines. The bacteria strains were taken from the Persian Type Culture Collection (PTCC). *Staphylococcus aureus* (PTCC No.: 1826) as a standard gram-positive bacterium and *E. coli* (PTCC No.: 1222) as a standard gram-negative bacterium were cultured in 10 mL LB broth medium in the shaker incubator at 150 rpm at 37°C for 18 - 24 h. Then 150 μL of 0.5 McFarland bacterial suspensions was cultured on LB plates. Then, disks of the samples (0.5 cm in diameter and sterilized under UV light for 1 h) were prepared, placed on the plates, and incubated at 37°C for 24 - 72 h. Finally, the inhibition zone of the nanofibers against each bacterium was measured.

The biological properties of SF nanofibers and 3DPH nano-scaffolds, such as cell attachment, proliferation and cell viability, were evaluated using a mouse fibroblastic cell line (L929) (National Cells Bank, Pasteur Institute of Iran). L929 cells were cultured in DMEM containing 10% FBS supplemented with penicillin (100 units/mL) and streptomycin (100 μg/mL) at 37°C, and humidified with 5% CO_2. Before the cell culture, the sample nanofibers were sterilized under UV light for an hour, placed in a 24-well culture plate, seeded with 10^4 cells on them, and incubated in a humidified atmosphere of 5% CO_2 at 37°C for 48 h. The nanoscaffolds samples were rinsed with PBS solution to remove the dissociative cells. The attached cells to scaffolds were fixed using 2.5% (v/v) glutaraldehyde solution for 3 h at 4°C. Then, the scaffolds were thoroughly washed with PBS solution, sequentially dehydrated in a graded ethanol series (30, 50, 70, 95, and 100% (v/v)) for 10 min, and dried. The FE-SEM was used for depicting the cell attachment on the nano-scaffolds.

Cell viability was evaluated at 1, 3, and 5 days of culture using MTT (3-(4, 5-dimethylthiazol-2-yl)-2, 5-diphenyl tetrazolium bromide) assay. The test was performed five times per sample (n = 5). Finally, the cell viability percentage was calculated using the following equation:

$$Cell\ viability\ (\%) = \frac{OD\ of\ the\ sample}{OD\ of\ the\ control\ group} \times 100$$

(1)

3.8. Statistical Analysis

The data were expressed as a mean ± standard deviation. Statistical analysis was performed using one-way analysis of variance (SPSS program, version 22). A P-value < 0.01 was considered as statistically significant.

4. Results

The surface morphology and size of synthesized nanoscffolds were measured using FE-SEM. According to our microscopic examination, the silk fibroin nanofibers had random orientation as well as straight, relatively smooth, and uniform fabrication with the average diameter of 137 ± 40 nm (Figure 2C).

Figure 2. A, Fabrication of nanofibrous scaffold by electrospinning method; B, The electrospun silk fibroin nanofiber mat; and C, Field emission scanning electron microscopy image of SF nanofibers

Three-dimensional (3D) and porous structure of 3DPH nano-scaffold manufactured by sodium alginate, ZnO-NPs and SF nanofibers is shown in Figure 3.

Antibacterial activity of 3DPH nano-scaffolds containing different concentrations of ZnO-NPs against *S. aureus* and *E. coli* bacteria was investigated by performing the disk diffusion assay. As shown in Figure 4 and Table 1, enhancing ZnO concentration encapsulated in nano-scaffolds increased the mean diameter of inhibition zone against both bacterial strains.

The cytotoxicity level of 3DPH nano-scaffolds comprising different ZnO-NPs concentrations through the viability level of mouse fibroblast cells (L929 cell line) was assessed using MTT test. The 3DPH nano-scaffolds free of ZnO-NPs (SF-SA/PEO) were considered as a control sample. As Figure 5 illustrates, the scaffolds did not induce cytotoxicity over three days of study. However, it was found that the cell viability and proliferation decreased by increasing the ZnO-NPs concentration compared with the control samples. According to our results, the cell viability was slightly affected by ZnO-NPs and increased from low concentrations to 1.5% (w/v) of zinc oxide so that almost 70% of the cells were alive over three days. However, the cell viability was significantly declined (P < 0.01) to 50% after three days of exposure to 2% ZnO-NPs-loaded 3DPH nano-scaffolds due to the release of more ZnO (Figure 5).

Moreover, L929 cell line (Figure 6A) was cultured on the SF nanofibers and 3DPH nano-scaffold containing 1.5% (w/v) ZnO-NPs to survey the cell interaction with the nanofiber surface. As FE-SEM images show, the cells were connected, and most of the nano-scaffolds' surface was covered by them (Figure 6B and C).

Finally, it was concluded that silk fibroin nanofibers were suitable for epidermal grafts, and 3DPH nano-scaffold loaded with ZnO-NPs were ideal for dermal grafts. Taking into account the promising results of biological analyses, it was determined that nanofibrous and 3DPH nano-scaffolds composite may have been suitable for skin dermo-epidermal grafts and skin regeneration.

5. Discussion

Chronic wounds (e.g., deep burns, pressure ulcers, venous ulcers, and metabolic disorders) significantly impact the patient's health, whose treatment is extremely important. There are several factors that contribute to the slow healing of chronic wounds, including the destruction of the ECM, a lack of stem cells, and a high risk of bacterial infections (13, 14). In this study, silk fibroin nanofiber was fabricated by using electrospinning (as an epidermal graft) and 3DPH nano-scaffold with composite of sodium alginate/ZnO-NPs solution as well as silk fibroin electrospun nanofibers by freeze-drying method (as a dermal graft). Due to their morphology, high porosity, and high surface area-to-volume ratio, nanofibrous scaffolds have wide applications in the fields of skin tissue engineering, artificial skin grafts, and wound dressing (15, 16). However, loading and releasing sensitive bioactive compounds such as antibiotics, DNA, proteins, nanoparticles, and other drugs into nanofibrous scaffolds is usually challenging (17). Hence, the drug's physicochemical properties, polymer choice, drug-polymer compatibility, drug-solvent compatibility, and formulation should be carefully considered for designing scaffolds. The complex interplay among various parameters significantly impacts the loading and sustainable drug release. Nano-scaffolds loaded with bioactive compounds such as ZnO-NPs can be employed as synthetic skin substitutes or tissue-engineered
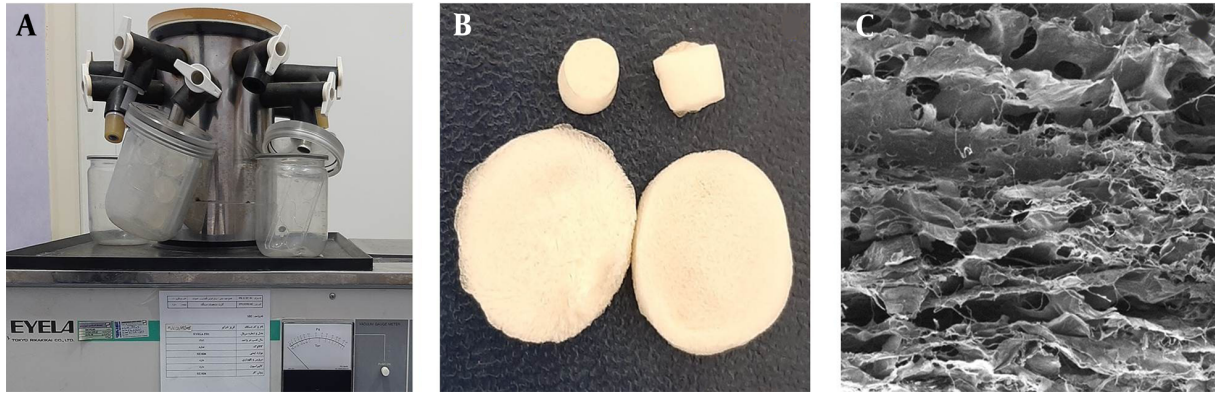
Figure 3. A, Fabrication of porous scaffolds by freeze-drying method; B, Film of three-dimensional porous hybrids nano-scaffold; and C, Field emission scanning electron microscopy image of 3DPH nano-scaffold
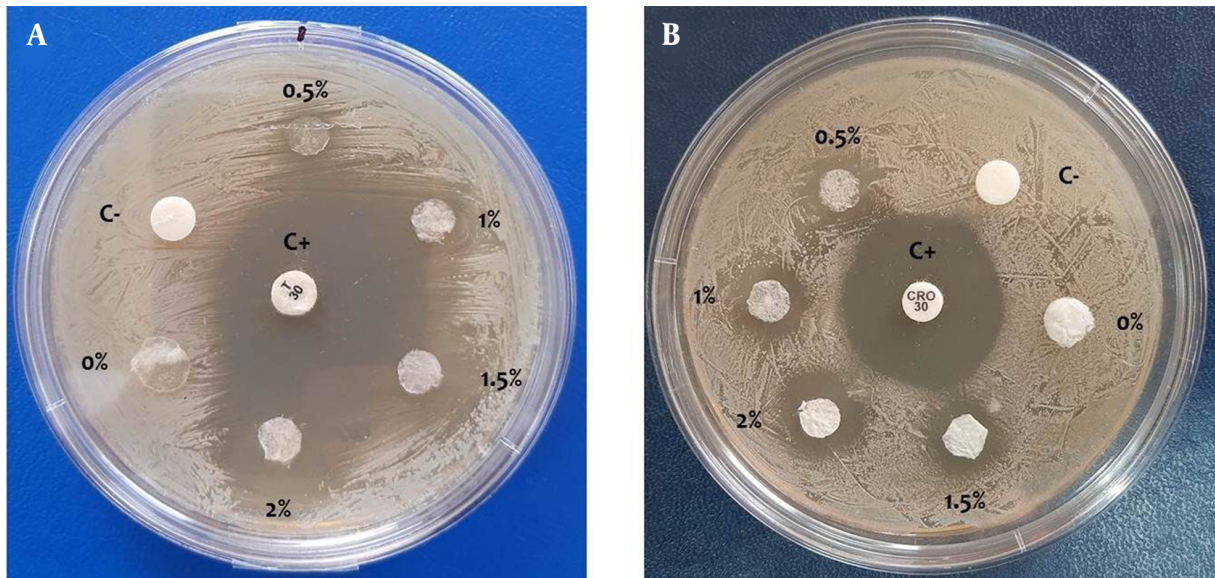

Figure 4. Antibacterial activity against A, *Staphylococcus aureus*; and B, *Escherichia coli* bacteria by three-dimensional porous hybrids nano-scaffolds containing 0, 0.5, 1, 1.5, and 2% (w/v) ZnO nanoparticles after 48 hours. Disks with and without antibiotic were considered positive (C⁺) and negative (C⁻) controls, respectively.

Table 1. Inhibition Zone of Three-dimensional Porous Hybrids (3DPH) Nano-scaffolds Loaded with Different Concentrations of ZnO Nanoparticles After 48 Hours [a]

Three-dimensional Porous Hybrids Nano-scaffolds with Different ZnO Nanoparticles Concentration (%)	Mean Inhibition Zone (mm)	
	Staphylococcus aureus	*Escherichia coli*
0	0	0
0.5	4 ± 0.7	4 ± 0.9
1	8 ± 1.2	6 ± 0.8
1.5	11 ± 1.3	7 ± 1
2	15 ± 0.9	9 ± 1.1

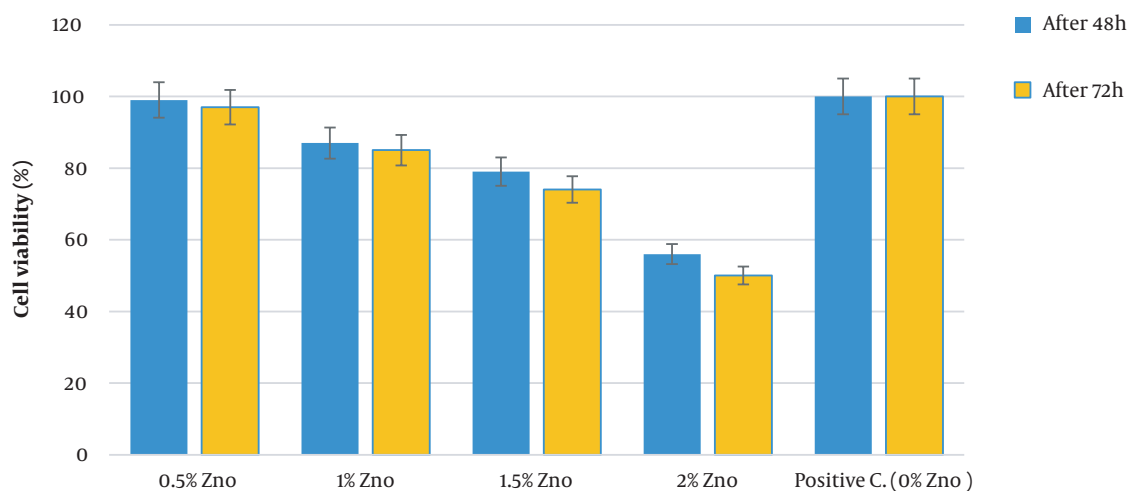[a] Values are mean ± standard error (n = 3).

Figure 5. L929 cell viability percentage on the three-dimensional porous hybrids nano-scaffolds incorporated with 0 (control), 0.5, 1, 1.5, and 2% (w/v) ZnO nanoparticles, assessed by the MTT assay after 2 and 3 days. * shows a statistically significant difference (P < 0.01).
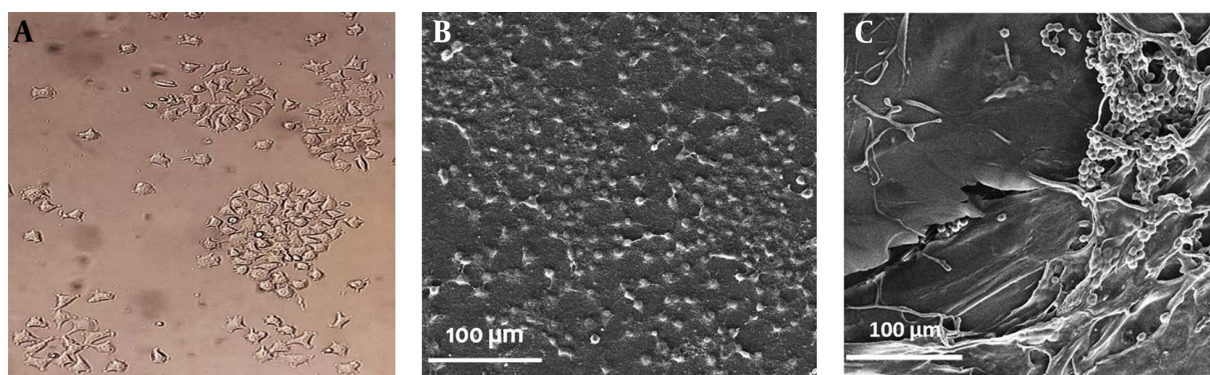

Figure 6. A, Morphology of L929 fibroblasts; B, Field emission scanning electron microscopy image of L929 fibroblasts cultured on silk fibroin nanofibers; and L929 C, Cell attachment to the three-dimensional porous hybrids scaffold after 72 h

artificial skin grafts (18, 19). Antibacterial properties of nano-scaffolds play a major role in accelerating wound treatment by decreasing the chance of bacterial colonization and infection (20, 21). Consequently, *S. aureus* is more sensitive to ZnO-NPs than *E. coli*, which was in agreement with the results from previous studies (22-24). The scaffolds used for wound healing should be non-toxic for the cells because cell migration, angiogenesis, and connective tissue regeneration can occur in the presence of biocompatible (non-toxic) wound dressings (25). However, higher concentration of zinc oxide may not be appropriate for cell attachment and viability, which was in line with the results from previous studies. According to these studies, high dosages of ZnO-NPs may have promoted oxidative stress and cell apoptosis (26, 27). Additionally, ZnO-NPs can be ef-

fective in treating chronic wounds by stimulating the proliferation and growth of fibroblastic cells, promoting collagen synthesis as the main substrate of ECM, and angiogenesis (28, 29). Our findings demonstrated that the 1.5% (w/v) ZnO-incorporated 3DPH nano-scaffold had a prompting effect on the L929 cell's proliferation and attachment without any cell toxicity, which was consistent with MTT assay results. According to our study results, moreover, it was suggested that the positive effect of zinc with appropriate concentration on cell proliferation, adhesion, ECM regulation, and metabolic processing may have stabilized the cell membranes and accelerated the wound healing (30). Similar results were reported for SF nanofibers and 3DPH nano-scaffold, making them a promising tool for wound healing and tissue engineering (31). There are a number

of research studies exploring the application of nanotechnology for synthesizing skin grafts. However, it should be noted that these studies are typically conducted in a laboratory setting and have not widely employed clinical practice. One study published in 2011 investigated the application of a nanofiber scaffold made from polyethylene glycol (PEG) and collagen for synthesizing skin grafts in a clinical setting (32). The study found that using nanofiber scaffold, compared to traditional skin grafts, accelerated the wound healing process and improved the skin regeneration. Another study examined a nanostructured hydrogel made from PEG and hyaluronic acid (HA) for synthesizing skin grafts in a clinical setting, and found that using nanostructured hydrogel improved skin regeneration and reduced scarring compared to traditional skin grafts (33).

5.1. Conclusions

In sum, silk fibroin nanofiber as an epidermal graft and 3DPH nano-scaffold loaded with ZnO-NPs as a dermal graft were fabricated. Examination of SEM images revealed the successful formation of fibrous and porous scaffold structures. The 1.5% (w/v) concentrations of ZnO-NPs were selected to incorporate into the 3DPH nano-scaffold. Antibacterial tests showed that the 3DPH nano-scaffold had the potential to inhibit the growth of gram-negative (*E. coli*) and gram-positive (*S. aureus*) bacteria. Taking into account the promising results of cytotoxicity and cell adhesion analyses, the nanofibrous and 3DPH nano-scaffolds composite may have been a suitable candidate for skin dermoepidermal grafts and skin regeneration.

Recommendations for future studies: Biocompatible and biodegradable natural polymers (silk fibroin and alginate) were used for the synthesis of scaffolds, which provided an excellent method to load and efficiently release the drugs (i.e., growth factors, antibiotics, and other bioactive compounds) effective in wound healing. In addition, they were cost-effective for mass production. However, it was suggested that further studies (e.g., mechanical tests of scaffolds and in vivo studies) should be carried out in this regard. Finally, the following were recommended for future studies:

(1) Development of 3D nano-scaffolds with loading of growth factors (EGF, FGF, VEGF, etc.) and other bioactive compounds effective in wound healing;

(2) Evaluation and optimization of nano-scaffold properties in vitro, including mechanical testing (i.e., tensile strength, Young's modulus, and elongation-to-break) and physicochemical tests (i.e., porosity, permeability, water uptake ability, water vapor transmission rate (WVTR));

(3) In vivo investigating the effect of nano-scaffolds (as skin tissue engineering and artificial skin grafts) on chronic wounds in laboratory animals.

Footnotes

References

1. Eming SA, Martin P, Tomic-Canic M. Wound repair and regeneration: mechanisms, signaling, and translation. *Sci Transl Med.* 2014;**6**(265):265sr6. [PubMed ID: 25473038]. [PubMed Central ID: PMC4973620]. https://doi.org/10.1126/scitranslmed.3009337.

2. Vig K, Chaudhari A, Tripathi S, Dixit S, Sahu R, Pillai S, et al. Advances in Skin Regeneration Using Tissue Engineering. *Int J Mol Sci.* 2017;**18**(4). [PubMed ID: 28387714]. [PubMed Central ID: PMC5412373]. https://doi.org/10.3390/ijms18040789.

3. Przekora A. A Concise Review on Tissue Engineered Artificial Skin Grafts for Chronic Wound Treatment: Can We Reconstruct Functional Skin Tissue In Vitro? *Cells.* 2020;**9**(7). [PubMed ID: 32640572]. [PubMed Central ID: PMC7407512]. https://doi.org/10.3390/cells9071622.

4. Kolimi P, Narala S, Nyavanandi D, Youssef AAA, Dudhipala N. Innovative Treatment Strategies to Accelerate Wound Healing: Trajectory and Recent Advancements. *Cells.* 2022;**11**(15). [PubMed ID: 35954282]. [PubMed Central ID: PMC9367945]. https://doi.org/10.3390/cells11152439.

5. Dixit S, Baganizi DR, Sahu R, Dosunmu E, Chaudhari A, Vig K, et al. Immunological challenges associated with artificial skin grafts: available solutions and stem cells in future design of synthetic skin. *J Biol Eng.* 2017;**11**:49. [PubMed ID: 29255480]. [PubMed Central ID: PMC5729423]. https://doi.org/10.1186/s13036-017-0089-9.

6. Varkey M, Ding J, Tredget EE. Advances in Skin Substitutes-Potential of Tissue Engineered Skin for Facilitating Anti-Fibrotic Healing. *J Funct Biomater.* 2015;**6**(3):547–63. [PubMed ID: 26184327]. [PubMed Central ID: PMC4598670]. https://doi.org/10.3390/jfb6030547.

7. Nathoo R, Howe N, Cohen G. Skin substitutes: an overview of the key players in wound management. *J Clin Aesthet Dermatol.* 2014;**7**(10):44–8. [PubMed ID: 25371771]. [PubMed Central ID: PMC4217293].

8. Kaur A, Midha S, Giri S, Mohanty S. Functional Skin Grafts: Where Biomaterials Meet Stem Cells. *Stem Cells Int.* 2019;**2019**:1286054. [PubMed ID: 31354835]. [PubMed Central ID: PMC6636521]. https://doi.org/10.1155/2019/1286054.

9. Savoji H, Godau B, Hassani MS, Akbari M. Skin Tissue Substitutes and Biomaterial Risk Assessment and Testing. *Front Bioeng Biotechnol.*

2018;**6**:86. [PubMed ID: 30094235]. [PubMed Central ID: PMC6070628]. https://doi.org/10.3389/fbioe.2018.00086.

10. Caballero Aguilar LM, Silva SM, Moulton SE. Growth factor delivery: Defining the next generation platforms for tissue engineering. *J Control Release*. 2019;**306**:40–58. [PubMed ID: 31150750]. https://doi.org/10.1016/j.jconrel.2019.05.028.

11. Nosrati H, Aramideh Khouy R, Nosrati A, Khodaei M, Banitalebi-Dehkordi M, Ashrafi-Dehkordi K, et al. Nanocomposite scaffolds for accelerating chronic wound healing by enhancing angiogenesis. *J Nanobiotechnology*. 2021;**19**(1):1. [PubMed ID: 33397416]. [PubMed Central ID: PMC7784275]. https://doi.org/10.1186/s12951-020-00755-7.

12. Vepari C, Kaplan DL. Silk as a Biomaterial. *Prog Polym Sci*. 2007;**32**(8-9):991–1007. [PubMed ID: 19543442]. [PubMed Central ID: PMC2699289]. https://doi.org/10.1016/j.progpolymsci.2007.05.013.

13. Bowers S, Franco E. Chronic Wounds: Evaluation and Management. *Am Fam Physician*. 2020;**101**(3):159–66. [PubMed ID: 32003952].

14. Falanga V, Isseroff RR, Soulika AM, Romanelli M, Margolis D, Kapp S, et al. Chronic wounds. *Nat Rev Dis Primers*. 2022;**8**(1):50. [PubMed ID: 35864102]. https://doi.org/10.1038/s41572-022-00377-3.

15. Tanzli E, Ehrmann A. Electrospun Nanofibrous Membranes for Tissue Engineering and Cell Growth. *Appl Sci*. 2021;**11**(15). https://doi.org/10.3390/app11156929.

16. Ye K, Kuang H, You Z, Morsi Y, Mo X. Electrospun Nanofibers for Tissue Engineering with Drug Loading and Release. *Pharmaceutics*. 2019;**11**(4). [PubMed ID: 30991742]. [PubMed Central ID: PMC6523318]. https://doi.org/10.3390/pharmaceutics11040182.

17. Luraghi A, Peri F, Moroni L. Electrospinning for drug delivery applications: A review. *J Control Release*. 2021;**334**:463–84. [PubMed ID: 33781809]. https://doi.org/10.1016/j.jconrel.2021.03.033.

18. Rayyif SMI, Mohammed HB, Curutiu C, Birca AC, Grumezescu AM, Vasile BS, et al. ZnO Nanoparticles-Modified Dressings to Inhibit Wound Pathogens. *Materials (Basel)*. 2021;**14**(11). [PubMed ID: 34200053]. [PubMed Central ID: PMC8200248]. https://doi.org/10.3390/ma14113084.

19. Khorasani MT, Joorabloo A, Adeli H, Milan PB, Amoupour M. Enhanced antimicrobial and full-thickness wound healing efficiency of hydrogels loaded with heparinized ZnO nanoparticles: In vitro and in vivo evaluation. *Int J Biol Macromol*. 2021;**166**:200–12. [PubMed ID: 33190822]. https://doi.org/10.1016/j.ijbiomac.2020.10.142.

20. Kaushik M, Niranjan R, Thangam R, Madhan B, Pandiyarasan V, Ramachandran C, et al. Investigations on the antimicrobial activity and wound healing potential of ZnO nanoparticles. *Appl Surf Sci*. 2019;**479**:1169–77. https://doi.org/10.1016/j.apsusc.2019.02.189.

21. Xie Y, He Y, Irwin PL, Jin T, Shi X. Antibacterial activity and mechanism of action of zinc oxide nanoparticles against Campylobacter jejuni. *Appl Environ Microbiol*. 2011;**77**(7):2325–31. [PubMed ID: 21296935]. [PubMed Central ID: PMC3067441]. https://doi.org/10.1128/AEM.02149-10.

22. Hadisi Z, Farokhi M, Bakhsheshi-Rad HR, Jahanshahi M, Hasanpour S, Pagan E, et al. Hyaluronic Acid (HA)-Based Silk Fibroin/Zinc

23. Oxide Core-Shell Electrospun Dressing for Burn Wound Management. *Macromol Biosci*. 2020;**20**(4). e1900328. [PubMed ID: 32077252]. https://doi.org/10.1002/mabi.201900328.

24. Becheri A, Dürr M, Lo Nostro P, Baglioni P. Synthesis and characterization of zinc oxide nanoparticles: application to textiles as UV-absorbers. *J Nanopart Res*. 2007;**10**(4):679–89. https://doi.org/10.1007/s11051-007-9318-3.

24. Bakhsheshi-Rad HR, Hamzah E, Ismail AF, Aziz M, Kasiri-Asgarani M, Ghayour H, et al. In vitro corrosion behavior, bioactivity, and antibacterial performance of the silver-doped zinc oxide coating on magnesium alloy. *Mater Corros*. 2017;**68**(11):1228–36. https://doi.org/10.1002/maco.201709597.

25. Dhivya S, Padma VV, Santhini E. Wound dressings - a review. *Biomedicine (Taipei)*. 2015;**5**(4):22. [PubMed ID: 26615539]. [PubMed Central ID: PMC4662938]. https://doi.org/10.7603/s40681-015-0022-9.

26. Feng P, Wei P, Shuai C, Peng S. Characterization of mechanical and biological properties of 3-D scaffolds reinforced with zinc oxide for bone tissue engineering. *PLoS One*. 2014;**9**(1). e87755. [PubMed ID: 24498185]. [PubMed Central ID: PMC3909231]. https://doi.org/10.1371/journal.pone.0087755.

27. Wilhelmi V, Fischer U, Weighardt H, Schulze-Osthoff K, Nickel C, Stahlmecke B, et al. Zinc oxide nanoparticles induce necrosis and apoptosis in macrophages in a p47phox- and Nrf2-independent manner. *PLoS One*. 2013;**8**(6). e65704. [PubMed ID: 23755271]. [PubMed Central ID: PMC3670863]. https://doi.org/10.1371/journal.pone.0065704.

28. Jiang J, Pi J, Cai J. The Advancing of Zinc Oxide Nanoparticles for Biomedical Applications. *Bioinorg Chem Appl*. 2018;**2018**:1062562. [PubMed ID: 30073019]. [PubMed Central ID: PMC6057429]. https://doi.org/10.1155/2018/1062562.

29. Augustine R, Dan P, Sosnik A, Kalarikkal N, Tran N, Vincent B, et al. Electrospun poly(vinylidene fluoride-trifluoroethylene)/zinc oxide nanocomposite tissue engineering scaffolds with enhanced cell adhesion and blood vessel formation. *Nano Res*. 2017;**10**(10):3358–76. https://doi.org/10.1007/s12274-017-1549-8.

30. Lansdown AB, Mirastschijski U, Stubbs N, Scanlon E, Agren MS. Zinc in wound healing: theoretical, experimental, and clinical aspects. *Wound Repair Regen*. 2007;**15**(1):2–16. [PubMed ID: 17244314]. https://doi.org/10.1111/j.1524-475X.2006.00179.x.

31. Patil PP, Reagan MR, Bohara RA. Silk fibroin and silk-based biomaterial derivatives for ideal wound dressings. *Int J Biol Macromol*. 2020;**164**:4613–27. [PubMed ID: 32814099]. [PubMed Central ID: PMC7849047]. https://doi.org/10.1016/j.ijbiomac.2020.08.041.

32. Liu Y, Li T, Han Y, Li F, Liu Y. Recent development of electrospun wound dressing. *Current Opinion in Biomedical Engineering*. 2021;**17**:100247. https://doi.org/10.1016/j.cobme.2020.100247.

33. Zhu J, Li F, Wang X, Yu J, Wu D. Hyaluronic Acid and Polyethylene Glycol Hybrid Hydrogel Encapsulating Nanogel with Hemostasis and Sustainable Antibacterial Property for Wound Healing. *ACS Appl Mater Interfaces*. 2018;**10**(16):13304–13316. [PubMed ID: 29607644]. https://doi.org/10.1021/acsami.7b18927.